Journal of Electroanalytical Chemistry 768 (2016) 62–71

Contents lists available at ScienceDirect

Journal of Electroanalytical Chemistry

journal homepage: www.elsevier.com/locate/jelechem

Effect of different additives with $-NH_2$ or $-NH_4^+$ functional groups on V(V) electrolytes for a vanadium redox flow battery

Gang Wang [a], Jichuan Zhang [a], Jie Zhang [a], Jinwei Chen [a], Shifu Zhu [a], Xiaojiang Liu [b], Ruilin Wang [a,*]

[a] College of Materials Science and Engineering, Sichuan University, Chengdu 610065, China
[b] Institute of Electronics Engineering, China Academy of Engineering Physics, Mianyang 621900, China

ARTICLE INFO

Article history:
Received 1 January 2016
Received in revised form 16 February 2016
Accepted 18 February 2016
Available online 22 February 2016

Keywords:
Vanadium redox flow battery
V(V) positive electrolyte
Organic amines and inorganic ammoniums additives
Stability
Electrochemical performance

ABSTRACT

Several organic amines with $-NH_2$ functional groups and inorganic ammoniums with $-NH_4^+$ functional groups have been comparatively investigated as stabilizers of the V(V) electrolyte for vanadium redox flow battery (VRB) to improve its stability and electrochemical performance. Thermal stability tests showed that chitosan (CTS) and nonionic-type polyacrylamide (NPAM) additives with $-NH_2$; ammonium thiocyanate (ATC), ferrous ammonium sulfate (FAS) and ammonium ferric sulfate (AFS) additives with $-NH_4^+$ could significantly improve the thermal stability of the V(V) electrolyte over a wide temperature range of −5 °C to 45 °C. The electrochemical behavior of the V(V) electrolyte with these preferred additives was further studied by cyclic voltammetry (CV), steady state polarization, electrochemical impedance spectroscopy (EIS) and charge–discharge test. The results indicated that the electrochemical activity and reversibility for the V(V) electrolyte with the best additive CTS with $-NH_4^+$ was significantly improved compared with the additives with $-NH_2$ and pristine one. In addition, the VRB employing the positive electrolyte with CTS exhibited excellent cycling stability and charge–discharge behavior with a high energy efficiency of 82.5%. The N-containing and O-containing functional groups of CTS in the V(V) electrolyte could modify the electrode and further improve the electrochemical performance and cycling stability of VRB.

1. Introduction

The redox flow battery system conceived by NASA in the 1970s [1] has risen considerably as an efficient large-scale Electrical Energy Storage (EES) approach, owing to its attractive features, such as flexible design, high safety, high efficiency and long cycle life.

As one of the most promising redox flow battery technologies for energy storage, The vanadium redox flow battery (VRB) pioneered by M. Skyllas-Kazacos [2] in the 1980s has been widely regarded as the most advanced and promising redox flow battery system, which overcomes the inherent problem of cross contamination in other redox flow batteries. By employing the V(V)/V(IV) and V(III)/V(II) redox couples in sulfuric acid as the positive and negative active species, respectively, the capacity and power output of VRB are dependent on the volume and concentration of the electrolyte [3–7]. However, the irreversible formation of hydrated V_2O_5 precipitates due to the poor solubility and thermal stability for V(V) species in sulfuric acid at elevated temperatures will decrease energy density of VRB and cripple the pump circulation and even damage the battery, that will greatly limit its application to energy storage and block its commercialization process in the field of large-scale EES [8,9].

The rate and extent of precipitation in the V(V) electrolyte were found to be mainly affected by the solution temperature, the vanadium concentration, the sulfuric acid concentration, the state of charge (SOC) of the electrolytes, and the type and quantity of stabilizers [10,11]. In the past years, many research works have been carried out to increase the stability of V(V) species in sulfuric acid and keep high concentration and wide temperature range mainly based on the factors above [12–33]. M. Skyllas-Kazacos group has done a lot of pioneering work on the stability of V(V) electrolyte. They found that the stability of V(V) electrolyte can be improved by increasing the concentration of sulfuric acid, decreasing the concentration of V(V) species to below 1.8 M, adjusting the temperature (10 °C to 40 °C) and adding appropriate stabilizers. However, the high concentration of sulfuric acid favors the precipitation of V(IV), V(III) and V(II) species [34] and also enhances the acid corrosion of battery materials, the concentration below 1.8 M would greatly decrease the energy density of battery [3], and the temperature controlled in a smaller range would limit the practical applications of VRB [35]. So adding stabilizers into V(V) electrolyte is thought to be one of the most effective and economic methods for delaying and even preventing the precipitate formation [36]. Organic additives, such as Coulter dispersants [22], carboxylic acids compounds [13,18,27,30], CHPTAC cationic etherifier [28], alcohols compounds containing –OH, −SH or $-NH_2$ groups with ring or chain structures at tertiary carbon atoms [13–17, 19–21,24–26,30]; inorganic additives, such as HCl [27], sodium

* Corresponding author.
E-mail address: rl.wang@scu.edu.cn (R. Wang).

http://dx.doi.org/10.1016/j.jelechem.2016.02.029
1572-6657/

pyrophosphate tetrabasic [29], $NH_4H_2PO_4$ [31], $(NH_4)_2SO_4 + H_3PO_4$ composite additives [32,33], were reported as promising stabilizers for V(V) electrolyte, which could inhibit the precipitation formation [13].

Among the reported additives, organic compounds with $-NH_2$ groups were a kind of efficient stabilizing agents, which could affect the stability and electrochemical performance of V(V) positive electrolyte and V(III) negative electrolyte, respectively. He et al. [23] employed a short-chain amine aminomethanesulfonic acid as additive to improve the thermal stability of V(V) electrolyte and charge–discharge and cycling performance of VRB. Liu et al. [37] investigated the effect of a short-chain amine L-aspartic acid on V(III) electrolyte and it was found that the addition of L-aspartic acid into the 2 M V(III) electrolyte can stabilize the electrolyte by delaying its precipitation and further improve the performance of battery. However, they focused on the short-chain amines with acid groups and didn't refer to the other kinds of organic amines such as long-chain amines, cyclic amines, amides and sulfonamides.

Moreover, Ding et al. [31] proposed that V(V) electrolyte with inorganic compounds $NH_4H_2PO_4$ exhibited a better electrochemical performance and battery performance compared with the other phosphate due to the formation of the complex between the additive and vanadium ion. Recently, M. Skyllas-Kazacos group [32,33] found that the combination of 2 wt% $(NH_4)_2SO_4$ + 1 wt% H_3PO_4 additives could significantly delay precipitation of V(V) electrolyte, and enhance energy density and performance of VRB.

So far, the reports on additives with $-NH_2$ and NH_4^+ groups for VRB electrolyte are few. Based on these facts, several different kinds of organic amines additives with $-NH_2$ groups and inorganic ammoniums additives with NH_4^+ groups were chosen to comparatively investigate the influence and corresponding mechanism of $-NH_2$ and NH_4^+ groups on the stability of V(V) electrolyte at a wide range of temperature.

2. Experimental

2.1. Preparation of V(V) electrolyte

The 1.8–2.8 M V(V)/5.0 M H_2SO_4 electrolyte solutions were prepared by electrolytic dissolution and reduction V_2O_5 (99.4%) in sulfuric acid in a two-compartment electrolysis cell [26–28]. The negative electrolysis cell employed the same concentration and volume of pristine sulfuric acid as the positive one. The sulfuric acid with the same concentration in the positive and negative electrolysis cell was separated by a cation exchange membrane. The concentration and valence of the vanadium ions in the electrolyte were measured by 916 Ti-Touch (Metrohm) potentiometric titrator.

2.2. Stability tests of V(V)

Stability tests of 2.8 M V(V) electrolytes with additives were performed in sealed glass tubes by *ex situ* heating/cooling treatment over a temperature range of −5 °C to 60 °C for 30 days. In order to investigate the additive effect on V(V) electrolyte, 0.5 wt% additive was added into the glass tube with electrolyte, which removed O_2 through piping N_2 for 5 min before starting test. All the tests were carried out statically and each sample was visually monitored and recorded more than twice a day for slight precipitation of V_2O_5. At the end of the 30-day test period, the electrolyte in the glass tube was filtered and the concentration of V(V) species was determined by potentiometric titrator analysis again.

2.3. Electrochemical behavior measurements

Cyclic voltammetry (CV) and steady polarization tests of 2.8 M V(V)/5.0 M H_2SO_4 electrolytes with and without additives were carried out using the CHI 600B electrochemical workstation (Shanghai Chenhua Instrument, China) at −5 °C, 25 °C and 45 °C. The test was performed based on a 3-electrode electrochemical cell employing graphite electrode as working electrode (surface area 3.14 mm^2), saturated mercurous sulfate electrode as reference electrode and platinum plate electrode as counter electrode. Before each test, the working electrode was manually polished with 0.3 μm and 0.5 μm α-Al_2O_3 power and then washed by ultrasonic cleaning in ethanol and distilled water for 5 min, respectively. Electrochemical impedance spectroscopy (EIS) was conducted by a Solartron 1287 electrochemical workstation (Solartron Metrology, the UK) at room temperature. The sinusoidal excitation voltage applied to the cells was 5 mV. The frequency range was from 0.01 Hz to 100 kHz.

2.4. Cell tests

As shown in Fig. 1, the internal structure of a single VRB cell was assembled by employing two pieces of graphite felts (Hunan Jiuhua Carbon Hi-Tech Co., Ltd.) with an active area of 30 cm^2 as electrodes, a PE-PSSA cation exchange membrane (Zhejiang Qianqiu Group Co., Ltd., China) as separator and two conductive graphite plates (Zibo Jinpeng Carbon Co., Ltd.) as current collectors. All the components above were sealed with fluorine rubber gasket. The external structure of the cell was composed of positive electrolyte, negative electrolyte, storage tank, pump, pipeline and gas. During the charge–discharge tests, 70 mL 1.8 M V(IV)/3.0 M H_2SO_4 electrolyte with 0.5 wt% additive and 70 mL 1.8 M V(III)/3.0 M H_2SO_4 electrolyte were used as the original positive and negative electrolyte, respectively, which were controlled by a peristaltic pump with a flow rate of 50 mL/min and circulating in the corresponding half-cell. Before tests, O_2 in the negative electrolyte was removed through piping N_2 for 5 min. The charge–discharge tests were conducted on CT2001A-5V/2A (Wuhan Land Co., China) between 0.8 V and 1.6 V at a current density of 50 mA cm^{-2}.

2.5. X-ray photoelectron spectroscopy (XPS)

X-ray photoelectron spectroscopy (XPS) of graphite felts was conducted on K-Alpha 1063 (Thermo Fisher Scientic, UK) with Al Kα X-ray source generated at 12 kV and 6 mA in an ultra-high vacuum of about 10^{-9} mBar. After the VRB cycling tests, the graphite felt electrode in the positive-half cell was took out and washed by deionized water and ultrasonic cleaning in deionized water to remove the electrolyte and impurities, and then dried in an oven at 120 °C for 2 h.

3. Results and discussion

3.1. Effect of additives on stability of V(V)

A certain amount (0.5 wt%) of several organic amines and inorganic ammoniums additives (Table 1) were employed to investigate the effect of $-NH_2$ and NH_4^+ on thermal stability of 2.8 M V(V)/5.0 M H_2SO_4 electrolyte from −5 °C to 60 °C.

Table 2 showed that the stability of pristine solution (without additives) decreased greatly as temperature rose from −5 °C to 60 °C, which was mainly due to the endothermic nature of the precipitation reaction for V(V) species [10]:

$$2VO_2^+ + H_2O \rightarrow V_2O_5 + 2H^+ \quad \Delta H > 0 \tag{1}$$

It was observed that the V(V) electrolyte with most of the additives could delay the precipitation reaction Eq. (1) and improve the stability of V(V) species compared with the pristine one at the same temperature. For example, the pristine solution suffered from precipitation within 30 days from −5 °C to 30 °C. After chitosan (CTS), sulfonamides (SA) or ammonium thiocyanate (ATC) was added, the V(V) solution was stable without any precipitation in 30 days from −5 °C to 30 °C, indicating that CTS, SA and ATC could improve the stability of the V(V) solution significantly. Other additives, such as nonionic-type polyacrylamide (NPAM), ferrous ammonium sulfate (FAS) and ammonium

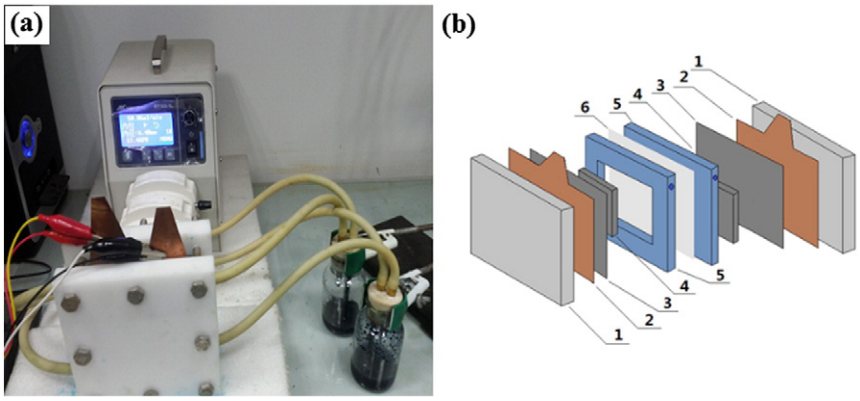

Fig. 1. (a) Picture of the single VRB cell and (b) a scheme of the cell configuration: 1—end plate, 2—current collector, 3—bipolar plate, 4—electrode, 5—electrolyte frame and 6—membrane.

ferric sulfate (AFS) could also improve the stability of the V(V) electrolyte to some extent from −5 °C to 45 °C.

To further investigate the additive effect on the V(V) solution, the concentration of V(V) species with and without additives was determined and recorded (Table 2) after 30 days at −5 °C, 10 °C and 30 °C, respectively. It was found that the concentration of all V(V) electrolytes decreased as the temperature increased. However, the concentration of V(V) species was improved after adding additives. These results were consistent with the thermal stability tests above. As shown in Table 2, the concentration of V(V) electrolytes with most of the additives remained 2.0 M after 30 days at low temperature, which was helpful to increase energy density and capacity over the current sulfate system of VRB [4]. For example, the concentration of electrolytes with CTS, SA, NPAM, FAS and AFS remained 2.0 M from −5 °C to 30 °C after 30 days. However, as a kind of normal alkane, the $-NH_2$ in octadecylamine (OA) was easily oxidized by the V(V) species and the electrolyte with OA maintained a lower concentration from −5 °C to 30 °C after 30 days. Similarly, the V(V) electrolyte with ammonium thiocyanate (ATC) also maintained a lower concentration, which was likely due to the formation of complex compound between thiocyanide and V(V) species. Although the V(V) solution with inorganic ammoniums additives ammonium sulfate (AS) and ammonium nitrate (AN) could maintain a higher concentration after 30 days at −5 °C, 10 °C and 30 °C, respectively, the precipitation was likely to occur within a shorter time compared with the one containing CTS, SA, NPAM, ATC, FAS and AFS. In general, the stability effect of the organic amines on the V(V) solution was better than the inorganic ammoniums. The concentration of V(V) electrolyte with good stabilizers such as CTS, SA, NPAM, ATC, FAS and AFS could be further improved through optimizing the quantity of addition.

Based on the results discussed above, it was indicated that organic amines CTS, SA, NPAM and inorganic ammoniums ATC, FAS and AFS as additives could significantly improve the stability of V(V) species and maintain a high concentration of V(V) solution at the same time. Researches have shown that appropriate additives could improve the thermal stability of V(V) electrolyte, which may be due to the interaction such as common ion effect, encapsulation, dispersion and, complexation and steric hindrance between the additives and V(V) species [22–31].

The organic amines compounds CTS, SA and NPAM and inorganic ammoniums compounds ATC, FAS and AFS can be used as promising stabilizers for V(V) electrolyte by further optimizing the quantity of addition and the range of temperature. Further investigations were conducted to verify the stability effect of these additives on V(V) electrolyte and then the corresponding stabilization mechanism was discussed.

3.2. Cyclic voltammetry

As seen in Fig. 2, all the CV curves of the electrolyte solutions with and without additives exhibited one couple of redox peaks towards to the redox reaction of V(V)/V(IV) couple. It was observed that the peak shape and peak position changed a little after adding 0.5 wt% additives, which would affect the reversibility of V(V)/V(IV) redox couple to some extent. The main differences were embodied in the parameters such as I_{pO} and I_{pR} (oxidation and reduction peak currents), I_{pO}/I_{pR} (ratio of oxidation peak current to reduction peak current) and ΔV_p (separation between the oxidation and reduction peak potential). It was observed that most of the additives could increase the I_{pO} and I_{pR}, decrease the ΔV_p and make the ratio of I_{pO}/I_{pR} close to one, which improved the reversibility of V(V)/V(IV) redox couple and electrode reaction kinetics at a certain extent [38]. Moreover, the effect of additives on the reversibility of V(V)/V(IV) redox couple was investigated by CV tests at a lower (−5 °C) and higher temperature (45 °C) and the ΔV_p ,I_{pO}/I_{pR} and peak currents were also recorded, respectively. Most of the organic amines and inorganic ammoniums additives could improve the reversibility of V(V)/V(IV) redox couple and electrode reaction kinetics at different temperature (Table 3). It was found that V(V)/V(IV) couple in electrolytes with organic amines additive CTS and inorganic ammoniums

Table 1
Molecular structures of studied organic amines and inorganic ammoniums additives.

Chemical name (short form)	Molecular structure	Chemical name (short form)	Molecular structure
Chitosan (CTS)	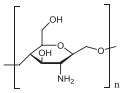	Ferrous ammonium sulfate (FAS)	$(NH_4)_2Fe(SO_4)_2$
Nonionic-type polyacrylamide (NPAM)		Ammonium ferric sulfate (AFS)	$NH_4Fe(SO_4)_2$
Sulfonamides (SA)	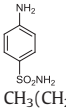	Ammonium thiocyanate (ATC)	NH_4SCN
Octadecylamine (OA)	$CH_3(CH_2)_{16}CH_2NH_2$	Ammonium sulfate (AS)	$(NH_4)_2SO_4$

Table 2
Effect of several organic amines and inorganic ammoniums additives on the thermal stability of 2.8 M V(V)/5.0 M H_2SO_4 electrolytes.

Additives (0.5 wt%)	Time to precipitation and concentration (M) of V(V) after 30 days (d) at different temperature (−5 °C, 10 °C and 30 °C)							
	−5 °C		10 °C		30 °C		45 °C	60 °C
CTS	>30 d	2.3 M	>30 d	2.1 M	>30 d	2.0 M	>30 d	11 d
NPAM	23 d	2.5 M	21 d	2.4 M	17 d	2.2 M	26 h	6 h
SA	>30 d	2.4 M	>30 d	2.1 M	>30 d	2.0 M	30 h	2 h
OA	26 d	2.0 M	22 d	1.8 M	19 d	1.5 M	16 h	1 h
FAS	26 d	2.6 M	24 d	2.4 M	21 d	2.2 M	27 h	1 h
AFS	25 d	2.5 M	23 d	2.3 M	20 d	2.1 M	26 h	1 h
ATC	>30 d	2.0 M	>30 d	1.8 M	>30 d	1.5 M	2 d	3 h
AS	24 d	2.4 M	20 d	2.1 M	17 d	2.1 M	25 h	1 h
Pristine	24 d	2.4 M	19 d	2.1 M	12 d	2.0 M	18 h	1 h

additive ATC exhibited the best electrochemical activity and reversibility, which would be further improved as temperature rose (Fig. 3), and the corresponding ΔV_p was reduced, the ratio of I_{pO}/I_{pR} was closer to one and oxidation and reduction peak currents were increased compared with the pristine one at the same temperature. Moreover, in order to further investigate the cyclic stability of V(V) electrolytes with CTS and ATC at a low and high temperature, 50 cycles continuous CV scans were conducted at a scan of 50 mV/s at −5 °C and 45 °C. The result of V(V) electrolytes with CTS and ATC showed good cycling stability with almost the same peak shape and peak position of CV curves (Fig. 4(a) and (b)). Similarly, the V(V) electrolytes with additives AFS, FAS and NPAM showed a better electrochemical reversibility and cyclic stability compared with the pristine one. –OH functional groups in CTS could interact with V(V) and V(IV) species at electrode surface, which accelerated the conversion between V(V) and V(IV) species and improved the electrochemical activity of V(V)/V(IV) redox couple [19]. In addition, for the additives CTS and ATC, the carbon atoms adjacent to nitrogen atoms in CTS possessed a high positive charge density to counterbalance the strong electronic affinity of the nitrogen atoms, analogously, ammonium radical in ATC also possessed a high positive charge density to counterbalance the strong electronic affinity of the thiocyanate radical, which could work as reaction active sites [37] for V(V)/V(IV) redox couple and further quicken the process of charge transfer. However, for the additive SA, the large conjugate system in its molecular structure could not supply extra reaction active sites for V(V)/V(IV) redox couple, which hindered the process of ion-exchange on electrode surface and finally lead to low electrochemical activity. While the additive NPAM with smaller conjugate system could supply more reaction active sites for V(V)/V(IV) redox couple compared with SA. Moreover, the additives AFS and FAS could also increase the electrochemical activity for V(V)/V(IV) redox couple, the corresponding mechanism would be analyzed in later mechanism discussion section. These results were consistent with the thermal stability tests above.

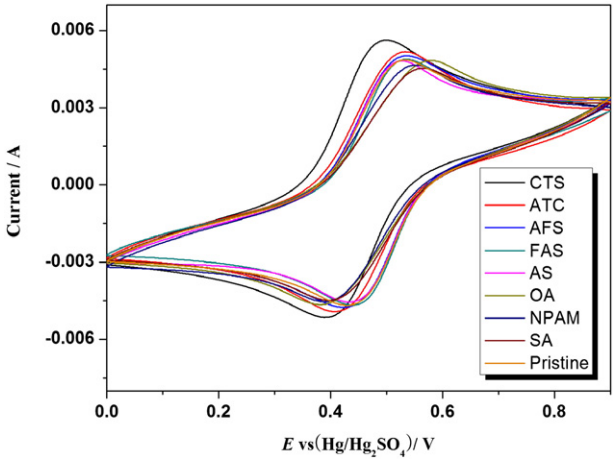

Fig. 2. CV curves of the electrolyte (2.8 M V(V)/5.0 M H_2SO_4) with 0.5 wt% organic amines and inorganic ammoniums additives on graphite electrode at room temperature at a scan rate of 50 mV s^{-1}.

A series of CV scans were carried out with scan rates from 10 ~ 100 mV/s to study the additive effect of 0.5 wt% CTS and ATC on the electrode reaction kinetics (Fig. 5(a) and (c)). As shown in Fig. 5(b) and (d), the calculation based on the plot of CV curves showed a good linear relationship between the square root of scan rates and the peak currents. The results above indicated a quasi-reversible and one-electron process for the redox reaction of V(V)/V(IV) couple, which agreed with the previous reports [20,28,34,35].

Theoretically, the value of the diffusion coefficient for a quasi-reversible reaction (D) is between that for a reversible one (D_1) and an irreversible one (D_2) [38]. For a reversible and irreversible one-step and one-electron reaction, the peak current i_p is given in Eqs. (2) and (3), respectively [39]:

$$i_p = 0.4463\left(F^3/RT\right)^{1/2} A C {D_1}^{1/2} \upsilon^{1/2} \text{ (reversible reaction)} \quad (2)$$

$$i_p = 0.4958\left(F^3/RT\right)^{1/2} \alpha^{1/2} A C {D_2}^{1/2} \upsilon^{1/2} \text{ (irreversible reaction)} \quad (3)$$

where F refers to the Faraday constant, R refers to the universal gas constant, T refers to the Kelvin temperature, A refers to the surface area of working electrode, C refers to the bulk concentration of primary reactant, D_1 and D_2 are the diffusion coefficients for a reversible and irreversible reaction, respectively. υ is the scanning rate. α is the transfer coefficient for a reversible reaction.

For a one-step and one-electron reaction at different temperature, the similar Eqs. of the peak current i_p can be deduced according to Eqs. (2) and (3). For example, when T = 25 °C = 298.15 K, Eqs. (2) and (3) can be transformed as follows:

$$i_p = 2.69 \times 10^5 A C {D_1}^{1/2} \upsilon^{1/2} \quad (4)$$

$$i_p = 2.99 \times 10^5 \alpha^{1/2} A C {D_2}^{1/2} \upsilon^{1/2} \quad (5)$$

For the one-step and one-electron quasi-reversible reaction-V(V)/V(IV) redox reaction, the diffusion coefficient D_1 and D_2 of V(V) species at different temperature according to Eqs. (2)–(5) and the known experimental conditions can be obtained from derivation and calculation.

As shown in Table 4, the diffusion coefficient of V(V) species in electrolyte increased with the rise of temperature, which indicated higher temperature could accelerate diffusion process of V(V) species at the electrode surface. The diffusion coefficients at different temperature for the test electrolytes were obtained and it was observed that the electrolytes with most of additives exhibited bigger diffusion coefficients than that of pristine one, which showed that additives could affect and accelerate the diffusion process of V(V) species at the electrode surface to a certain extent. For example, the diffusion rate of V(V) species in the electrolytes with CTS and ATC was significantly improved. The diffusion coefficient of V(V) species with CTS and ATC was increased from 6.15–7.57 × 10^{-7} (pristine) to 1.20–1.48 × 10^{-6} and 6.47–7.96 × 10^{-7}

Table 3
CV curves data of the electrolytes (2.8 M V(V)/5.0 M H_2SO_4) with 0.5 wt% organic amines and inorganic ammoniums additives at different temperature on graphite electrode.

Temperature (°C)	Additives	CTS	ATC	AFS	FAS	AS	OA	NPAM	SA	Pristine
−5	ΔV_p (V)	0.16	0.18	0.18	0.19	0.20	0.22	0.21	0.23	0.19
	I_{pO}/I_{pR}	0.98	1.02	1.03	1.04	1.03	1.04	1.05	1.05	1.03
25	ΔV_p (V)	0.11	0.13	0.12	0.11	0.11	0.19	0.16	0.17	0.13
	I_{pO}/I_{pR}	1.04	1.03	1.05	1.05	1.05	1.06	1.06	1.09	1.05
45	ΔV_p (V)	0.09	0.11	0.13	0.12	0.11	0.13	0.14	0.15	0.16
	I_{pO}/I_{pR}	1.01	1.02	1.04	1.05	1.08	1.10	1.09	1.13	1.06

at 25 °C, respectively. The similar results were also found for V(V) species with AFS, FAS and NPAM, which was agreed with the thermal stability and CV tests above.

3.3. Steady state polarization

Other kinetic parameters refer to V(V)/V(IV) redox reaction such as polarization resistance, exchange current density and electrochemical reaction rate constant were measured by steady state polarization and calculated based on Eq.(6) [20].

$$R_p = \frac{\eta}{i_0},\quad i_0 = \frac{RT}{nFR_p}, k_0 = \frac{i_0}{nFC_0} \tag{6}$$

where i_0 refers to the exchange current density, R refers to the universal gas constant, T refers to the Kelvin temperature, n refers to the number of electrons transferred in the reaction, F refers to the Faraday constant, R_p refers to the polarization resistance, k_0 refers to rate constant and C_0 refers to the solution concentration.

As shown in Fig. 6, the steady polarization curves for 2.8 M V(V)/5.0 M H_2SO_4 with test solutions exhibited an approximate straight line and so the corresponding parameters such as polarization resistance, exchange current density and electrochemical reaction rate constant could be obtained based on Eq. (6). Table 5 showed that as the temperature increased, the polarization resistance decreased, the exchange current density and electrochemical reaction rate constant increased, which indicated that the kinetic process of V(V) species at the electrode surface was accelerated. In addition, the kinetic process of V(V) species would be accelerated after adding most of the test additives. Taking 0.5 wt% CTS and ATC for example, the polarization resistance of the electrolytes with these two additives decreased from 4.67 Ωcm^2 (pristine) to 3.57 Ωcm^2 and 3.81 Ωcm^2 at 25 °C, respectively. While the exchange current density of the test samples with these two additives increased from 5.50 mA cm^{-2} (pristine) to 7.20 mA cm^{-2} and 6.74 mA cm^{-2}, and the corresponding electrochemical reaction rate constant increased

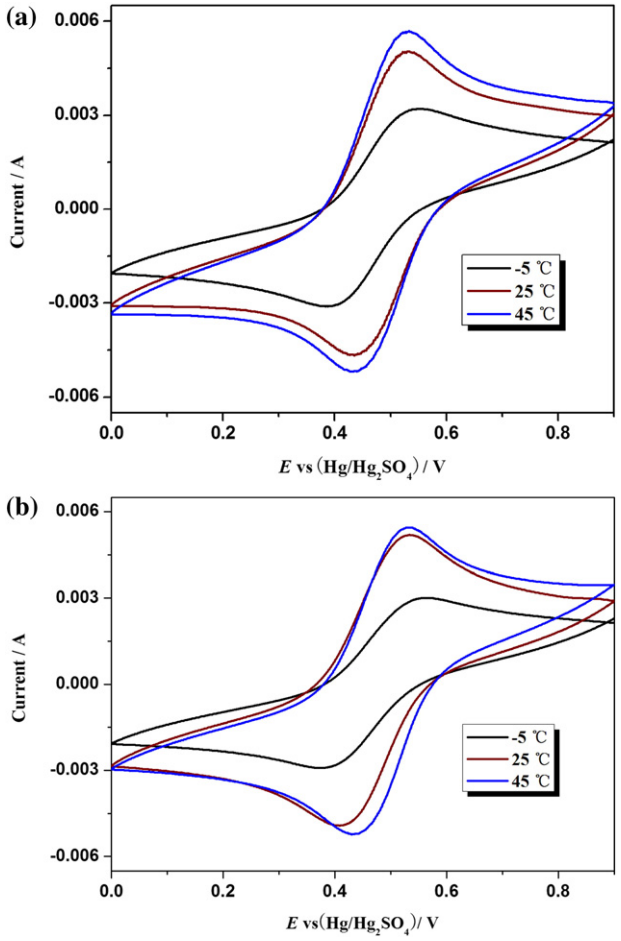

Fig. 3. CV curves of the electrolyte (2.8 M V(V)/5.0 M H_2SO_4) with (a) 0.5 wt% CTS and (b) 0.5 wt% ATC on graphite electrode at different temperature at a scan rates of 50 mV s^{-1}.

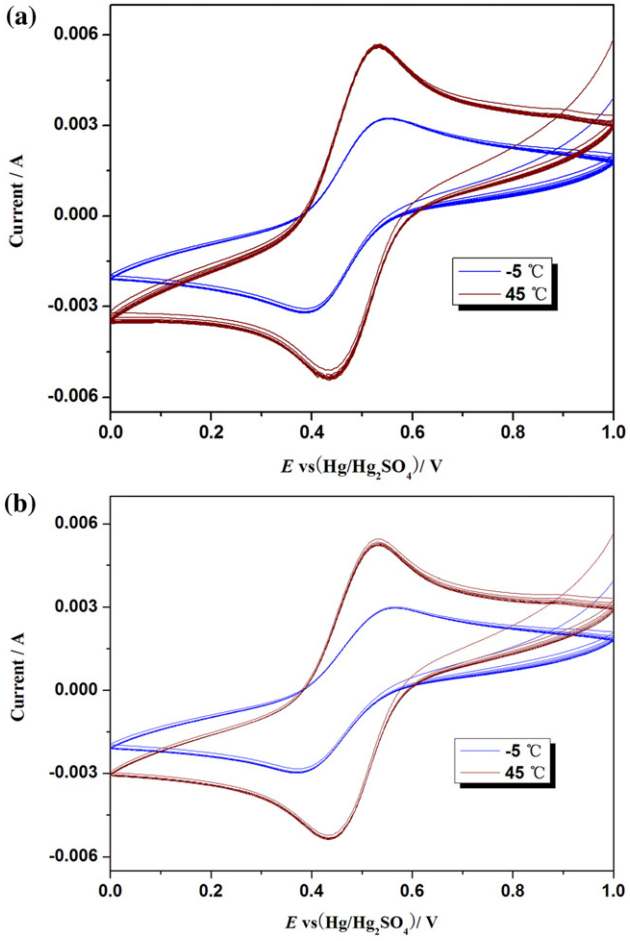

Fig. 4. CV curves (50 cycles) of the electrolyte (2.8 M V(V)/5.0 M H_2SO_4) with (a) 0.5 wt% CTS and (b) 0.5 wt% ATC on graphite electrode at −5 °C and 45 °C at a scan rate of 50 mV s^{-1}.

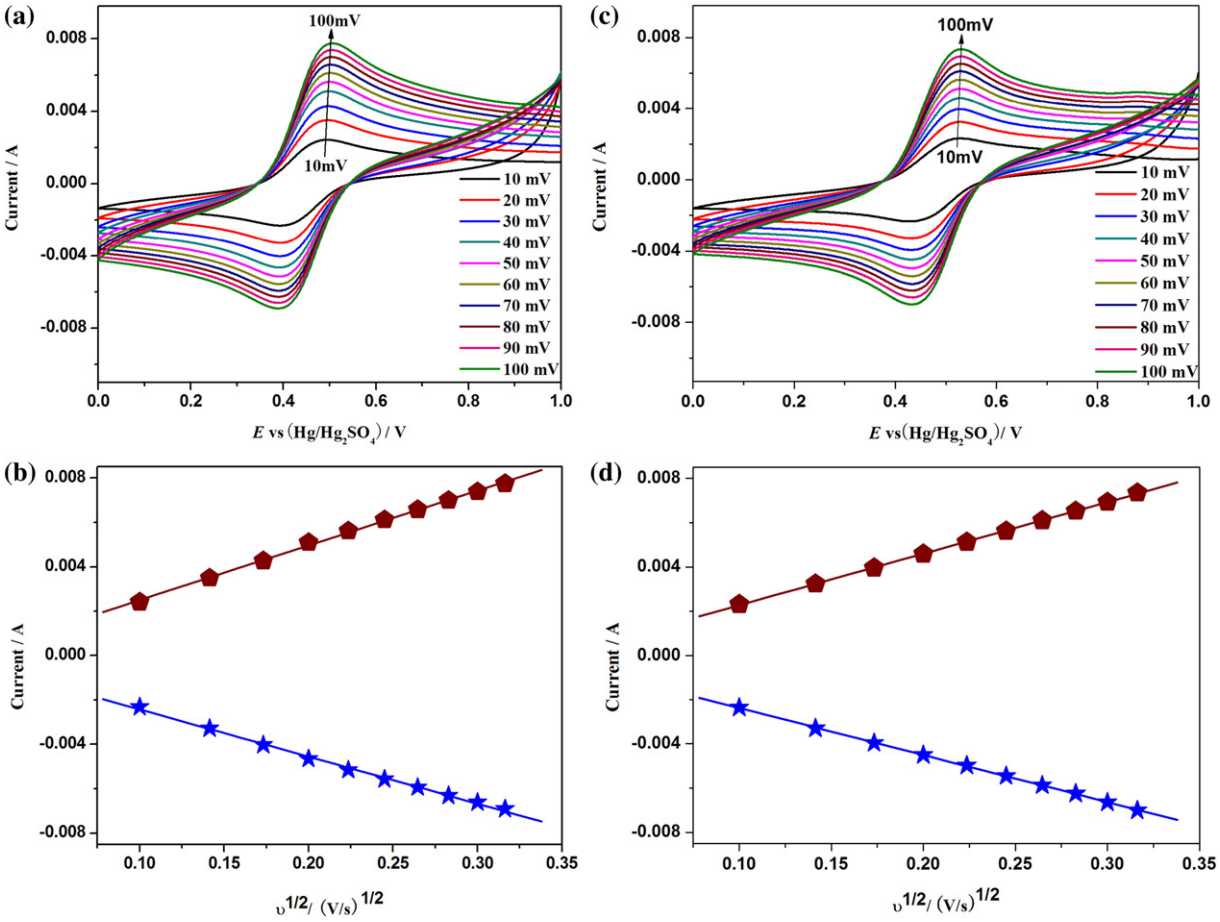

Fig. 5. (a) CV curves of the electrolyte (2.8 M V(V)/5.0 M H_2SO_4) with 0.5 wt% CTS on graphite electrode at room temperature at different scan rates and (b) corresponding relationship of oxidation and reduction current peak as a function of the square root of scan rate. (c) CV curves of the electrolyte (2.8 M V(V)/5.0 M H_2SO_4) with 0.5 wt% ATC on graphite electrode at room temperature at different scan rates and (d) corresponding relationship of oxidation and reduction current peak as a function of the square root of scan rate.

from 2.04×10^{-5} cm s^{-1} (pristine) to 2.67×10^{-5} cm s^{-1} and 2.49×10^{-5} cm s^{-1} at 25 °C, respectively. Analogously, the additives AFS, FAS and NPAM could also affect and accelerate kinetic process for V(V) species at the electrode surface to a certain degree.

3.4. Electrochemical impedance spectroscopy

Electrochemical impedance spectra were used to further investigate the charge transfer and diffusion process for the redox reaction of V(V)/V(IV) couple in the electrolyte (2.8 M V(V)/5.0 M H_2SO_4) at 25 °C. The Nyquist plots of the test solutions exhibited a semicircle in the high frequency region and a sloped line in the low frequency region, that indicated the redox reaction was affected and controlled by charge transfer process (at high frequency) and diffusion process (at low frequency), respectively (Fig. 7). And the equivalent circuit of these Nyquist plots was fitted and the corresponding parameters were obtained by Zsimpwin software. In the equivalent circuit, R_1 is the resistance composed of solution resistance, electrode resistance and the contact resistance. R_2 and W refer to the charge transfer resistance and Warburg diffusion impedance in the electrochemical process, respectively. CPE refers to the constant phase element represents the electric double-layer capacitance of the electrode/solution interface [19–21]. As shown in Table 6, the simulation results indicated that most of additives could improve charge transfer process and accelerate

Table 4
Effect of organic amines and inorganic ammoniums additives on the diffusion coefficient D_1 and D_2 of V(V) species.

Additives (0.5 wt%)	Diffusion coefficient D_1 (cm^2 s^{-1}) and D_2 (cm^2 s^{-1}) of V(V) species with different additives at different temperature								
	−5 °C			25 °C			45 °C		
	D_1	D_2	Error (%)	D_1	D_2	Error (%)	D_1	D_2	Error (%)
CTS	6.72×10^{-7}	5.45×10^{-7}	4	1.48×10^{-6}	1.20×10^{-6}	2	2.11×10^{-6}	1.71×10^{-6}	3
ATC	3.69×10^{-7}	2.99×10^{-7}	3	7.96×10^{-7}	6.47×10^{-7}	5	9.56×10^{-7}	7.74×10^{-7}	4
AFS	3.25×10^{-7}	2.64×10^{-7}	2	7.82×10^{-7}	6.35×10^{-7}	4	9.11×10^{-7}	7.40×10^{-7}	3
FAS	2.94×10^{-7}	2.39×10^{-7}	3	7.67×10^{-7}	6.23×10^{-7}	3	8.84×10^{-7}	7.18×10^{-7}	4
AS	2.65×10^{-7}	2.15×10^{-7}	5	7.44×10^{-7}	6.05×10^{-7}	4	8.29×10^{-7}	6.74×10^{-7}	2
OA	2.42×10^{-7}	1.97×10^{-7}	4	7.03×10^{-7}	5.71×10^{-7}	3	8.01×10^{-7}	6.51×10^{-7}	3
NPAM	2.28×10^{-7}	1.85×10^{-7}	3	6.91×10^{-7}	5.61×10^{-7}	2	7.86×10^{-7}	6.39×10^{-7}	4
SA	2.14×10^{-7}	1.74×10^{-7}	3	6.75×10^{-7}	5.48×10^{-7}	3	7.59×10^{-7}	6.14×10^{-7}	4
Pristine	2.78×10^{-7}	2.26×10^{-7}	4	7.57×10^{-7}	6.15×10^{-7}	4	8.47×10^{-7}	6.86×10^{-7}	5

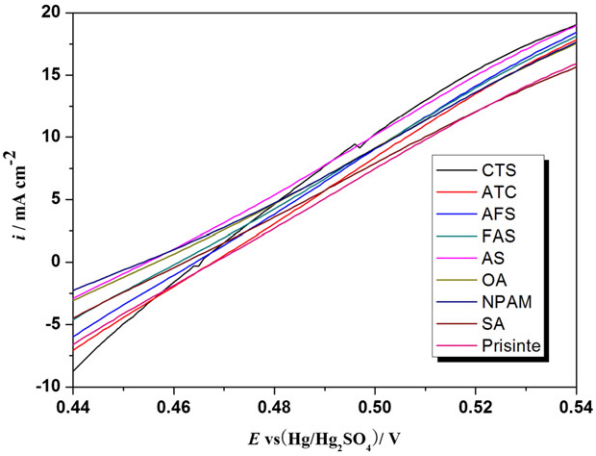

Fig. 6. Steady polarization curves for 2.8 M V(V)/5.0 M H_2SO_4 solution with 0.5 wt% organic amines and inorganic ammoniums additives on graphite electrode at a scan rate of 1 mV s^{-1}.

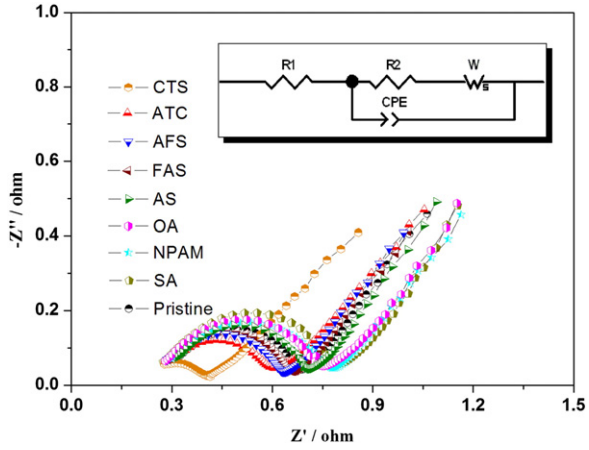

Fig. 7. Nyquist plots of the electrolytes with and without organic amines and inorganic ammoniums additives at room temperature.

diffusion process for the redox reaction of V(V)/V(IV) couple. Taking CTS for example, the R_1 and R_2 of V(V) species with 0.5 wt% CTS decreased from 0.2624 Ω cm^2 (pristine) to 0.2143 Ω cm^2 and 0.4194 Ω cm^2 (pristine) to 0.1980 Ω cm^2, respectively, that showed a faster charge transfer process. In addition, the parameter $Y_{0,2}$ for the electrolyte with CTS increased and exhibited a lower diffusion impedance compared with the pristine one, indicating a faster diffusion process. The similar results could also be found for the redox reaction of V(V)/V(IV) couple in V(V) electrolytes with 0.5 wt% CTS, ATC, AFS, FAS and NPAM.

3.5. Charge and discharge tests

The charge–discharge tests were commonly employed to characterize the performance of VRB, from which we could obtain a lot of important information of the battery such as coulombic, voltage and energy efficiency and cycling stability. Fig. 8 showed the charge–discharge curves and different efficiencies of a single VRB cell employing the positive electrolytes with and without test additives at 25 °C. And it was observed that most of additives could improve the performance of VRB compared with the pristine one. Taking the VRB with 0.5 wt% CTS (the best additive) for example, coulombic efficiency increased from 92.3% (pristine) to 94.3%, voltage efficiency increased from 84.6% (pristine) to 87.5% and energy efficiency increased from 78.1% (pristine) to 82.5%, respectively. The analogous results could also be found for ATC, AFS, FAS and NPAM, which was consistent with the thermal stability, CV, line polarization and electrochemical impedance spectra tests. It was likely due to that the preferred additives blocked the aggregation of the V(V) ions and reduced V_2O_5 precipitation and thus increased the efficiency of VRB.

Table 6
Parameters resulting from fitting the impedance plots with the equivalent circuit model in Fig. 7.

Additives (0.5 wt%)	R_1/Ω cm^2	CPE/S s^{-n} cm^{-2}		R_2/Ω cm^2	W, $Y_{0,2}$/S s^{-5} cm^{-2}
		$Y_{0,1}$	n		
CTS	0.2143	3.246×10^{-3}	0.9394	0.1980	3.259
ATC	0.2564	2.603×10^{-3}	0.8105	0.3413	2.664
AFS	0.2578	2.531×10^{-3}	0.7987	0.3846	2.485
FAS	0.2584	2.514×10^{-3}	0.7872	0.3921	2.402
AS	0.2633	2.457×10^{-3}	0.7654	0.4202	2.337
OA	0.2701	2.443×10^{-3}	0.7390	0.4591	2.218
NPAM	0.2805	2.418×10^{-3}	0.7185	0.5157	2.096
SA	0.2822	1.952×10^{-3}	0.6963	0.5575	1.876
Pristine	0.2624	2.461×10^{-3}	0.7724	0.4194	2.358

Moreover, cycling stability tests of VRB with the best additive CTS and the pristine one were comparatively performed at the current density of 50 mA cm^{-2} at 25 °C (Fig. 9). It was observed that after 30 cycles, the coulombic (93.5%), voltage (86.5%) and energy efficiency (80.9%) of VRB with CTS could also maintain a high level compared with the 1st cycle, which was better than that of the pristine one.

3.6. X-ray photoelectron spectroscopy

X-ray photoelectron spectroscopy was used to further investigate the surface of positive graphite felt electrode after cycling test of VRB

Table 5
Kinetic parameters by way of steady polarization for 2.8 M V(V)/5.0 M H_2SO_4 solution with organic amines and inorganic ammoniums additives on graphite electrode at different temperature.

Additives (0.5 wt%)	Kinetic parameters for V(V) solution with different acid additives at different temperature								
	−5 °C			25 °C			45 °C		
	R_p (Ω cm^2)	i_0 (mA cm^{-2})	k_0 (10^{-5} cm s^{-1})	R_p (Ω cm^2)	i_0 (mA cm^{-2})	k_0 (10^{-5} cm s^{-1})	R_p (Ω cm^2)	i_0 (mA cm^{-2})	k_0 (10^{-5} cm s^{-1})
CTS	5.58	4.14	1.53	3.57	7.20	2.67	2.52	10.88	4.03
ATC	5.87	3.94	1.46	3.81	6.74	2.49	2.80	9.79	3.62
AFS	5.97	3.87	1.43	4.01	6.41	2.37	3.08	8.90	3.29
FAS	6.22	3.71	1.37	4.29	5.99	2.22	3.32	8.26	3.06
AS	6.68	3.46	1.28	4.69	5.48	2.03	3.47	7.90	2.92
OA	6.77	3.41	1.26	4.72	5.44	2.01	3.54	7.74	2.86
NPAM	6.85	3.37	1.25	4.78	5.37	1.99	3.59	7.64	2.83
SA	6.91	3.34	1.24	4.80	5.35	1.98	3.62	7.57	2.80
Pristine	6.54	3.53	1.31	4.67	5.50	2.04	3.45	7.95	2.94

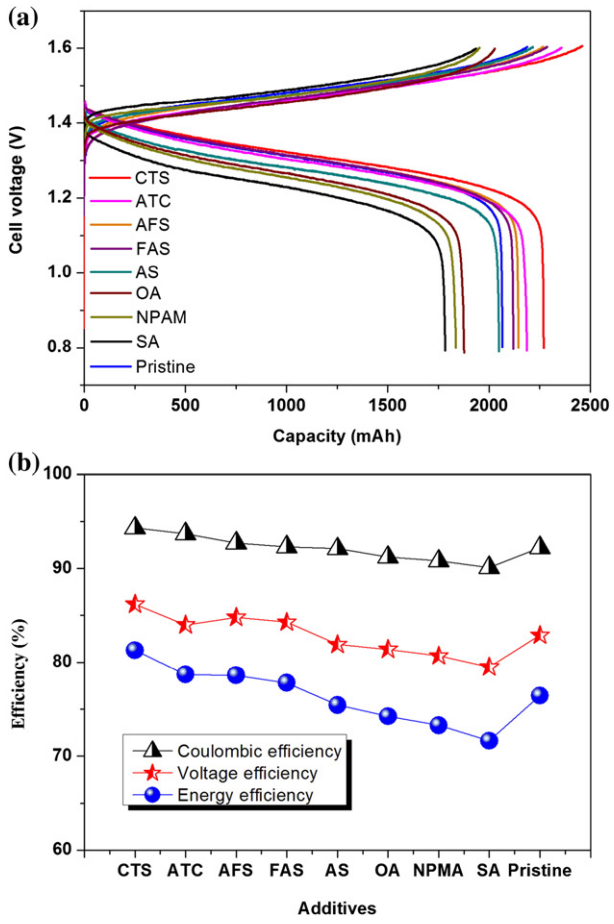

Fig. 8. (a) Charge–discharge curves and (b) different efficiency for VRB employed electrolyte with organic amines and inorganic ammoniums additives at current density of 50 mA cm^{-2} at room temperature.

employing electrolyte with the best additive CTS compared with the pristine one. The XPS spectra were performed in the binding energy charge of 1–1100 eV and the corresponding results were shown in Fig. 10 and Table 7. It was observed that there were three groups of evident energy peaks on 286, 534 and 403 eV, referring to carbon (C), oxygen (O) and nitrogen (N), respectively, which verified the existence of

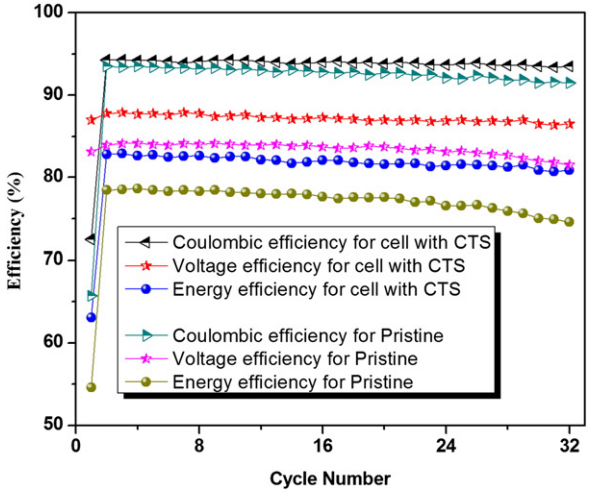

Fig. 9. Columbic, voltage and energy efficiency of VRB in cycling tests with and without 0.5 wt% CTS.

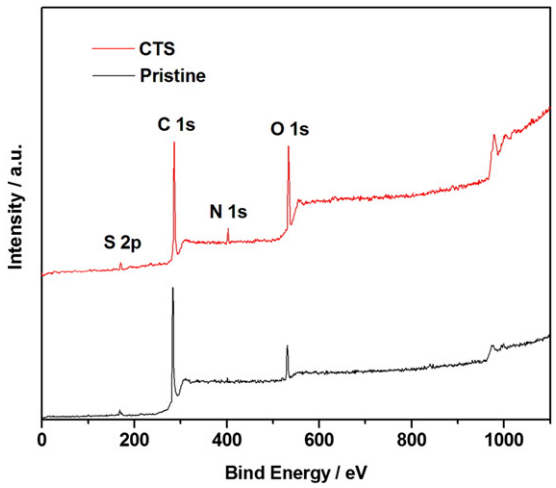

Fig. 10. XPS spectra of graphite felt in the positive electrolyte with and without 0.5 wt% CTS after cycling tests.

–OH and quaternary N functional groups in CTS [28]. The quaternary N functional groups here were transformed from $–NH_2$ functional groups of CTS in acid electrolyte as follows:

Comparing with the pristine one, more C atoms in CTS were oxidized and transformed to O-containing functional groups, resulting in a weak C 1s peak with a content of 52.35% and a strong O 1s peak with a content of 39.28%, meantime, the additive CTS could supply extra N atoms to transform more N-containing functional groups, causing a strong N 1s peak with a content of 5.75%. The more O-containing and N-containing functional groups could provide more active sits for the V(V)/V(IV) redox reaction at the surface of graphite felt electrode and improve the hydrophilic property of graphite felt [19,28], and further accelerate the electrochemical process. In addition, the loss of O-containing and N-containing functional groups during cycling tests could be supplemented by the additive CTS and the cycling stability could also be enhanced [37].

3.7. Mechanism discussion

The enhanced electrochemical performance for VRB resulted from the addition of CTS, ATC, AFS, FAS and NPAM should be fundamentally ascribed to the increased reaction active sites for V(V)/V(IV) redox couple. Herein, these good additives play the roles of electron mediators and quicken the process of charge transfer for V(V)/V(IV) redox reaction:

$$VO_2^+ + 2H^+ + e^- \underset{\text{(additives)}}{\overset{\text{electron mediators}}{\rightleftharpoons}} VO^{2+} + 2H_2O$$

Jin et al. [40] proposed the catalytic mechanism of NGS for V(V)/V(IV) redox reaction. Although the mechanism was different from the one originally proposed by Sun et al. [41], we think it could also be used for explaining the effect of additives on V(V) solution by appropriate adjustment. As shown in Scheme 1, the relatively high negative

Table 7
The relative contents of the elements on the surface of graphite felt after cycling tests.

Element	Peak binding energy (eV)	CTS (atom %)	Pristine (atom %)
S 2p	170.50	2.62	2.50
C 1s	286.20	52.35	76.42
N 1s	403.20	5.75	1.51
O 1s	533.85	39.28	19.57

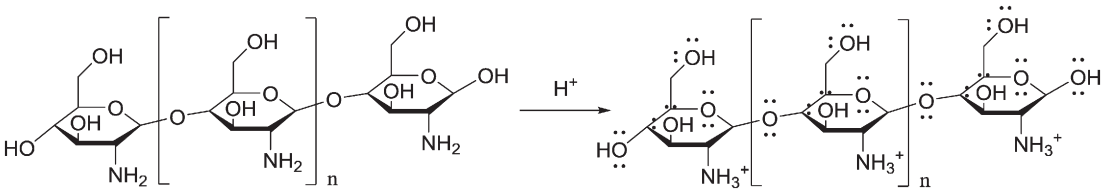

Scheme 1. The conversion of CTS in acid positive electrolyte.

charge density of the D due to its rich electrons could promote the adsorption process of positively charged reactant ions, including VO_2^+ and VO^{2+} on the active sites. Furthermore, the additional electrons of D could create localized states at the surface of the graphite electrode, which may match the empty molecular orbital of VO_2^+ or VO^{2+} to form a D–V transitional state and facilitate the electron transportation between the reactants and the additives. During the redox reaction process, with the electrode potential negatively (positively) shifted, the electron on the electrode transfers into (out off) the antibonding orbital of VO_2^+ (VO^{2+}) through D–V bonding. For the reduction process, the additional electron in the antibonding orbital of VO_2^+ weakens the VO bond and removes one of the oxygens with two protons. While for the oxidation process, one H_2O molecule coordinates with the empty orbital of VO^{2+} to generate a VO_2^+ and two protons. Lastly, the VO^{2+} or VO_2^+ is removed from the active site. Among the four steps, Jin et al. [40] think that the first step is the rate-determining step for both the oxidation process and reduction process. The consistent results with cycle voltammetry, steady state polarization and electrochemical impedance spectra in this paper could be explained by replacing D with O or N atom for additives CTS, ATC, AFS, FAS and NPAM in Scheme 2. In acid positive electrolyte, the $-NH_2$ groups of CTS would convert $-NH_3^+$ groups (Scheme 1), playing the role of A^+ in Scheme 2, while the O atom of CTS with a lot of lone pair electrons, playing the role of D^- in Scheme 2, which could supply a large number of reaction active sites for V(V)/V(IV) redox couple and quicken the process of charge transfer. The additive NPAM with $-NH_2$ groups in acid positive electrolyte would result in a similar effect. For the additive ATC, the NH_4^+ and SCN^- played the role of A^+ and D^-, respectively. While for the additives AFS and FAS, both the NH_4^+ and iron ions played the role of A^+, the SO_4^{2-} played the role of D^-. The analysis above based on Scheme 2 could be used for analyzing and explaining the previous experimental results. However, when some results could not be explained by this mechanism, the original mechanism proposed by Sun et al. could be used for supplement.

4. Conclusion

The stability and electrochemical behavior of the V(V) electrolyte with and without several organic amines with $-NH_2$ functional groups and inorganic ammoniums with $-NH_4^+$ functional groups were studied and compared. The results showed that the organic amines compounds CTS and NPAM and inorganic ammoniums compounds ATC, FAS and AFS could significantly improve the stability of V(V) electrolyte from −5 °C to 45 °C. Comparing with the pristine one, these preferred additives could improve the electrochemical performance of V(V)/V(IV) redox couple to some extent. Overall, the effect of the organic amines on the V(V) solution was better than the inorganic ammoniums. Among these compounds, the additive CTS with $-NH_2$ and –OH groups could significantly improve the electrochemical activity and reversibility for the redox reaction of V(V)/V(IV) couple, and the VRB employed CTS exhibited a high energy efficiency and cycling stability. CTS with $-NH_2$ could be used for promising stabilizers for V(V) positive electrolyte in VRB application, while the other preferred additives needed to be further optimized. The effect mechanism of $-NH_2$ and NH_4^+ groups in the preferred additives on the stability of V(V) electrolyte was proposed and discussed.

Acknowledgments

All authors herein are grateful to the support from National Science Foundation of China (NSFC, Project No. 21306119); Provincial Natural Science Foundation of Sichuan (2013FZ0034, 2013JY0150); Outstanding Young Scientist Foundation of Sichuan University (2013SCU04A23); Dongfang Electric Corporation (13H0844) and China Academy of Engineering Physics (HG2012039, KF13007).

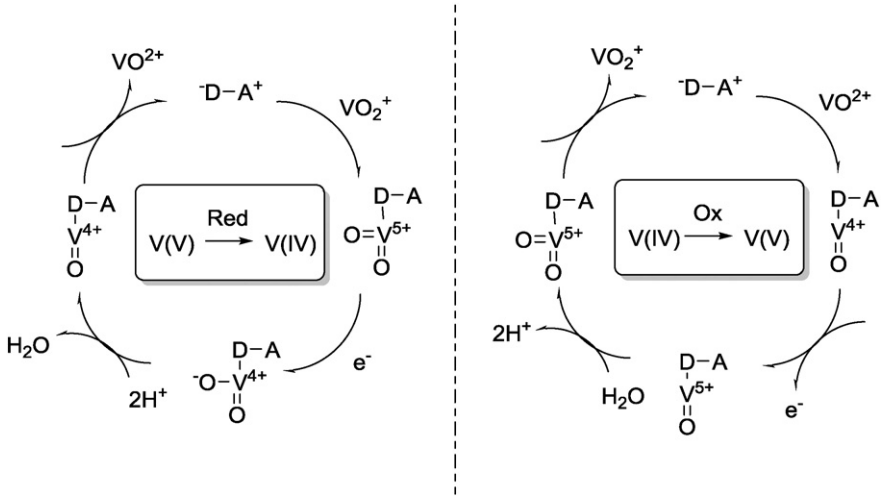

Scheme 2. Possible catalytic mechanism of additives (D: electron-rich atoms or groups for donating electrons, A: electron-poor atoms or groups for accepting electrons) for the V(V)/V(IV) redox reaction.

References

[1] Redox Flow Cell Development and Demonstration Project, NASA TM-79067, US: Department of Energy 1979, pp. 245–253.
[2] M. Skyllas-Kazacos, R. G. Robins, AU Patent 0,575,247 (1986)
[3] M. Skyllas-Kazacos, M.H. Chakrabarti, S.A. Hajimolana, F.S. Mjalli, M. Saleem, J. Electrochem. Soc. 158 (2011) R55–R79.
[4] Z.G. Yang, J.L. Zhang, M.C.W. Kintner-Meyer, X.C. Lu, D.W. Choi, J.P. Lemmon, J. Liu, Chem. Rev. 111 (2011) 3577–3613.
[5] P.K. Leung, X. Li, C. Ponce de Léon, L. Berlouis, C.T.J. Low, F.C. Walsh, RSC Adv. 2 (2012) 10125–10156.
[6] G. Kear, A.A. Shah, F.C. Walsh, Int. J. Energy Res. 36 (2011) 1105–1120.
[7] M.J. Watt-Smith, H. Al-Fetlawi, P. Ridley, R.G.A. Wills, A.A. Shah, F.C. Walsh, J. Chem. Technol. Biot. 88 (2013) 126–138.
[8] M. Skyllas-Kazacos, G. Kazacos, G. Poon, H. Verseema, Int. J. Energy Res. 34 (2010) 182–189.
[9] M. Vijayakumar, L.Y. Li, G. Graff, J. Liu, H.M. Zhang, Z.G. Yang, J.Z. Hu, J. Power, Sources 196 (2011) 3669–3672.
[10] F. Rahman, M. Skyllas-Kazacos, J. Power, Sources 189 (2009) 1212–1219.
[11] M. Kazacos, M. Cheng, M. Skyllas-Kazacos, J. Appl. Electrochem. 20 (1990) 463–467.
[12] M. Skyllas-kazacos, AU Patent 8,800,472 (1989).
[13] M. Kazacos, M.Skyllas-Kazacos, US Patent 7,078,123 (2006).
[14] M. Skyllas-Kazacos, US Patent 6,143,443 (2000).
[15] M. Skyllas-Kazacos, M. Kazacos, A. Mohammed, WO Patent 9,512,219 (1994).
[16] M. Kazacos, M. Skyllas-Kazacos, US Patent 6,468,688 (2002).
[17] M. Skyllas-Kazacos, M. Kazacos, US Patent 6,562,514 (2003).
[18] J.L. Zhang, L.Y. Li, Z.M. Nie, B.W. Chen, M. Vijayakumar, S. Kim, W. Wang, B. Schwenzer, J. Liu, Z.G. Yang, J. Appl. Electrochem. 41 (2011) 1215–1221.
[19] S. Li, K.L. Huang, S.Q. Liu, D. Fang, X.W. Wu, D. Lu, T. Wu, Electrochim. Acta 56 (2011) 5483–5487.
[20] X.J. Wu, S.Q. Liu, N.F. Wang, S. Peng, Z.X. He, Electrochim. Acta 78 (2012) 475–482.
[21] Z.J. Jia, B.G. Wang, S.Q. Song, X. Chen, J. Electrochem. Soc. 159 (2012) A843–A847.
[22] F. Chang, C.W. Hu, X.J. Liu, L. Liu, J.W. Zhang, Electrochim. Acta 60 (2012) 334–338.
[23] Z.X. He, J.L. Liu, H.G. Han, Y. Chen, Z. Zhou, S.G. Zheng, W. Lu, S.Q. Liu, Z. He, Electrochim. Acta 106 (2013) 556–562.
[24] S. Peng, N.F. Wang, C. Gao, Y. Lei, X.X. Liang, S.Q. Liu, Y.N. Liu, Int. J. Electrochem. Sci. 7 (2012) 4314-–44321.
[25] S. Peng, N.F. Wang, C. Gao, Y. Lei, X.X. Liang, S.Q. Liu, Y.N. Liu, Int. J. Electrochem. Sci. 7 (2012) 4388–4396.
[26] G. Wang, J.W. Chen, X.Q. Wang, J. Tian, H. Kang, X.J. Zhu, Y. Zhang, X.J. Liu, R.L. Wang, J. Electroanal. Chem. 709 (2013) 31–38.
[27] G. Wang, J.W. Chen, X.Q. Wang, J. Tian, H. Kang, X.J. Zhu, Y. Zhang, X.J. Liu, R.L. Wang, J. Energy Chem. 23 (2014) 73–81.
[28] G. Wang, J.W. Chen, Y.D. Xu, B.C. Yan, X.Q. Wang, X.J. Zhu, Y. Zhang, X.J. Liu, R.L. Wang, RSC Adv. 4 (2014) 63025–63035.
[29] S.K. Park, J. Shima, J.H. Yang, C.S. Jin, B.S. Lee, Y.S. Lee, K.H. Shin, J.D. Jeon, Electrochim. Acta 121 (2014) 321–327.
[30] H.G. Han, Z.X. He, J.L. Liu, Y. Chen, S.Q. Liu, Ionics (2014) 1–8.
[31] C. Ding, X. Ni, X.F. Li, X.L. Xi, X.W. Han, X.H. Bao, H.M. Zhang, Electrochim. Acta 164 (2015) 307–314.
[32] S. Roe, C. Menictas, M. Skyllas-Kazacos, J. Electrochem. Soc. 163 (2016) A5023–A5028.
[33] N. Kausar, A. Mousa, M. Skyllas-Kazacos, Chemelectrochem. (2015), http://dx.doi.org/10.1002/celc.201500453.
[34] F. Rahman, M. Skyllas-Kazacos, J. Power, Sources 72 (1998) 105–110.
[35] M. Skyllas-Kazacos, C. Menictas, J. Electrochem. Soc. 143 (1996) L86–L88.
[36] M. Skyllas-Kazacos, M. Rychick, R. Robins, US Patent 4,786,567 (1988).
[37] J.L. Liu, S.Q. Liu, Z.X. He, H.G. Han, Y. Chen, Electrochim. Acta 130 (2014) 314–321.
[38] F. Huang, Q. Zhao, C.H. Luo, G.X. Wang, K.P. Yan, D.M. Luo, Chin. Sci. Bull. 57 (2012) 4237–4243.
[39] A.J. Bard, L.R. Faulkner, Electrochemical Methods—Fundamentals and Applications, 6Wiley, New York, 2001 231–236.
[40] J.T. Jin, X.G. Fu, Q. Liu, Y.R. Liu, Z.Y. Wei, K.X. Niu, J.Y. Zhang, ACS Nano 7 (2013) 4764–4773.
[41] B. Sun, M. Skyllas-Kazacos, Electrochim. Acta 37 (1992) 2459–2465.